Eur. Phys. J. C 56, 267–277 (2008)
DOI 10.1140/epjc/s10052-008-0643-1

THE EUROPEAN PHYSICAL JOURNAL C

Regular Article – Theoretical Physics

Lepton polarization asymmetry and forward–backward asymmetry in exclusive $B \to K_1 \tau^+ \tau^-$ decay in universal extra dimension scenario

Asif Saddique[1,2], M. Jamil Aslam[3,4,a], Cai-Dian Lü[3]

[1] Department of Physics, Quaid-i-Azam University, Islamabad, Pakistan
[2] National Centre for Physics, Islamabad, Pakistan
[3] Institute of High Energy Physic, P.O. Box 918(4), Beijing, 100049, P.R. China
[4] Department of Physics, COMSATS Institute of Information Technology, Chak Shahzad Campus, Islamabad, Pakistan

Received: 9 March 2008 / Revised version: 7 May 2008 /
Published online: 27 June 2008 –

Abstract. Decay rate, forward–backward asymmetry and polarization asymmetries of the final state leptons in $B \to K_1 \tau^+ \tau^-$, where K_1 is the axial vector meson, are calculated in the standard model and in the universal extra dimension (UED) model. The sensitivity of the observables to the compactification radius R, the only unknown parameter in the UED model, is studied. Finally, the helicity fractions of the final state K_1 are calculated and their dependence on the compactification radius is discussed. This analysis of the helicity fraction is briefly extended to $B \to K^* \ell^+ \ell^-$ $(\ell = e, \mu)$ and compared with the other approaches existing in the literature.

1 Introduction

It is generally believed that the standard model (SM) of particle physics is one of the most successful theories of the second half of the previous century in explaining the data observed so far, but no one can say that it is the end of physics. Intensive search for physics beyond the SM is now being performed in various areas of particle physics, which is expected to get direct evidence at high energy colliders such as the Large Hadron Collider (LHC). During the last years there has been increased interest in models with extra dimensions, since they solve the hierarchy problem and can provide a unified framework of gravity and other interactions together with a connection with string theory [1–6]. Among them a special role play the ones with universal extra dimensions (UED), as in these models all SM fields are allowed to propagate in all available dimensions. The economy of UED models is that there is only one new free parameter in addition to the SM, the radius R of the compactified extra dimension. Now, above the compactification scale $1/R$ a given UED model becomes a higher dimensional field theory whose equivalent description in four dimensions consists of SM fields, the towers of their Kaluza–Klein (KK) partners and additional towers of KK modes having no partner in the SM. The Appelquist, Cheng and Dobrescu (ACD) model [7], with one extra universal dimension, is the simplest model of this type. In this model the only additional free parameter relative to the SM is the compactification scale $1/R$. Thus, all the masses of the KK particles and their interactions with SM particles and also among themselves are described in terms of $1/R$ and the parameters of the SM [8, 9].

The most profound property of the ACD model is the conservation of KK parity, which implies the absence of a tree level contribution of KK states to the low energy processes taking place at a scale $\mu \ll 1/R$. This brings about interest in the flavor-changing-neutral-current (FCNC) transitions $b \to s$, as these are not allowed at tree level but are induced by the Glashow–Iliopoulos–Miani (GIM) amplitudes [10] at the loop level in the SM and hence the one loop contribution due to KK modes to them could in principle be important. These processes are used to constrain the mass and couplings of the KK states, i.e. the compactification parameter $1/R$ [11].

Buras et al. have computed the effective Hamiltonian of several FCNC processes in the ACD model, particularly in the b sector, namely $B_{s,d}$ mixing and a $b \to s$ transition such as $b \to s\gamma$ and $b \to s\ell^+\ell^-$ [8, 9]. The implications of physics with UED are being examined with the data from accelerator experiments; for example, from Tevatron experiments the bound on the inverse of the compactification radius is found to be about $1/R \geq 300\,\text{GeV}$ [12]. Exclusive $B \to K(K^*)\ell^+\ell^-$, $B \to K(K^*)\nu\bar{\nu}$ and $B \to K^*\gamma$ decays are analyzed in the ACD model, and it was shown that the uncertainties connected with hadronic matrix elements do not mask the sensitivity to the compactification parameter, and the current data on the decay rates of $B \to K^*\gamma$ and $B \to K^*\ell^+\ell^-$ $(\ell = e, \mu)$ can provide a simi-

[a] e-mail: jamil@ncp.edu.pk

lar bound to the inverse compactification radius: $1/R \geq$ 300–400 GeV [13]. In addition to these the decay modes $B \to K_1 \ell^+ \ell^-$ $(\ell = e, \mu)$, $B \to \phi \ell^+ \ell^-$, $B \to \gamma \ell^+ \ell^-$ and $\Lambda_b \to \Lambda \ell^+ \ell^-$ have also been considered, with the possibility of observing such processes at hadron colliders [14–17]. Very recently, Haisch et al. have reexamined the constraints on universal extra dimension models arising from inclusive radiative $\bar{B} \to X_s \gamma$ decay [18]. They took leading order contributions due to exchange of Kaluza–Klein modes as well as the available next-to-next-to-leading order corrections to the $\bar{B} \to X_s \gamma$ branching ratio in the SM. For the large flat universal extra dimension, they obtained a lower bound on the inverse of the compactification radius $1/R > 600$ GeV and that is independent of the Higgs mass.

Colangelo et al. have also considered another set of observables in FCNC transitions, namely those of the inclusive $B \to X_s +$ leptons and exclusive $B \to K(K^*) +$ leptons decay modes, where the leptons are $\tau^+ \tau^-$ [19]. There are no experimental data on these days as yet; however, as first noticed in [20], these processes are of great interest due to the possibility of measuring lepton polarization asymmetries which are sensitive to the structure of the interactions, so that they can be used to test the SM and its extensions. They analyzed the τ^- polarization asymmetries in a single universal extra dimension model both for inclusive and exclusive semileptonic B meson decays. Besides this, they investigated another observable, the fraction of longitudinal K^* polarization in $B \to K^* \ell^+ \ell^-$, for which a new measurement in two bins of momentum transfer to the lepton pair is available in the case of $\ell = e, \mu$. They studied the dependence of this quantity on the compactification parameter, for $B \to K^* \tau^+ \tau^-$ and in the case of light leptons, together with the fraction of K^* polarization in the same modes, and discussed the possibility to constrain the universal extra dimension scenario.

In this work, we will study spin effects on $B \to K_1 \tau^+ \tau^-$ in the ACD model using the framework of $B \to K^* \tau^+ \tau^-$ described by Colangelo et al. [19]. We investigate the branching ratio, forward–backward and polarization asymmetries for the final state τ^-. Although the sensitivity of the branching ratio and forward–backward asymmetry on the extra dimension is mild, we still believe that together with the τ^- lepton polarization asymmetries, these can be used to provide additional constraints on the compactification parameter. In extension to this, we have also discussed the fraction of longitudinal K^* polarization in $B \to K^* \ell^+ \ell^-$, for which new measurements in two bins of momentum transfer to the lepton pair is available in the case of $\ell = e, \mu$ and compared them with the other approaches existing already in the literature [19]. Finally, we have used the same method to calculate the helicity fractions of K_1 in $B \to K_1 \ell^+ \ell^-$ both in the SM and in the ACD model. We hope that these fractions put other useful constraints on the universal extra dimension scenario.

The paper is organized as follows. In Sect. 2 we present the effective Hamiltonian for $B \to K_1 \ell^+ \ell^-$ in the ACD model. In Sect. 3, we will calculate the decay rate and forward–backward asymmetry for $B \to K_1 \tau^+ \tau^-$. Sections 4 and 5 deal with the study of polarization asymmetries of the final state τ^- and the helicity fractions of the final state K_1 meson, respectively. We will summarize our results in the last section.

2 Effective Hamiltonian

At the quark level the decay $B \to K_1 \ell^+ \ell^-$ is the same as $B \to K^* \ell^+ \ell^-$, as discussed by Ali et al. [21], i.e. $b \to s \ell^+ \ell^-$, and it can be described by an effective Hamiltonian obtained by integrating out the top quark and $W^\pm$ bosons:

$$H_{\rm eff} = -4 \frac{G_{\rm F}}{\sqrt{2}} V_{tb} V_{ts}^* \sum_{i=1}^{10} C_i(\mu) O_i(\mu) \,, \tag{1}$$

where the O_i are four local quark operators and the C_i are Wilson coefficients calculated in the naive dimensional regularization (NDR) scheme [22].

One can write the above Hamiltonian in the following free quark decay amplitude:

$$\begin{aligned} &\mathcal{M}(b \to s \ell^+ \ell^-) = \\ &\quad \frac{G_{\rm F} \alpha}{\sqrt{2}\pi} V_{tb} V_{ts}^* \Big\{ C_9^{\rm eff} [\bar{s} \gamma_\mu L b][\bar{\ell} \gamma^\mu \ell] + C_{10} [\bar{s} \gamma_\mu L b][\bar{\ell} \gamma^\mu \gamma^5 \ell] \\ &\quad - 2 \hat{m}_b C_7^{\rm eff} \left[\bar{s} {\rm i} \sigma_{\mu\nu} \frac{\hat{q}^\nu}{\hat{s}} R b \right] [\bar{\ell} \gamma^\mu \ell] \Big\} \,, \end{aligned} \tag{2}$$

with $L/R \equiv \frac{(1 \mp \gamma_5)}{2}$, and where $s = q^2$ which is just the momentum transfer from heavy to light meson. The amplitude given in (2) contains long distance effects encoded in the form factors and short distance effects that are hidden in the Wilson coefficients. These Wilson coefficients have been computed at next-to-next-to-leading order (NNLO) in the SM [23–30]. Specifically for exclusive decays, the effective coefficient $C_9^{\rm eff}$ can be written as

$$C_9^{\rm eff} = C_9 + Y(\hat{s}) \,, \tag{3}$$

where the perturbatively calculated result of $Y(\hat{s})$ is [22]

$$\begin{aligned} Y_{\rm pert}(\hat{s}) = {} & g(\hat{m}_c, \hat{s})(3C_1 + C_2 + 3C_3 + C_4 + 3C_5 + C_6) \\ & - \frac{1}{2} g(1, \hat{s})(4C_3 + 4C_4 + 3C_5 + C_6) \\ & - \frac{1}{2} g(0, \hat{s})(C_3 + 3C_4) + \frac{2}{9}(3C_3 + C_4 + 3C_5 + C_6) \,. \end{aligned} \tag{4}$$

Here the hat denotes the normalization in terms of the B meson mass. For the explicit expressions of the g and the numerical values of the Wilson coefficients appearing in (4), we refer to [22].

Now the new physics effects manifest themselves in rare B decays in two different ways, either through a new contribution to the Wilson coefficients or through the new operators in the effective Hamiltonian, which are absent in the SM. In the ACD model the new physics comes about through the Wilson coefficients. Buras et al. have computed the above coefficients at NLO in the ACD model including the effects of KK modes [8, 9]; we use these results

to study $B \to K_1\tau^+\tau^-$ decay like the one done in the literature for $B \to K^*(K_1)\mu^+\mu^-$ [13,14]. As has already been mentioned, the ACD model is the minimal extension of the SM with only one extra dimension and it has no extra operator other than the SM; therefore, the whole contribution from all the KK states is in the Wilson coefficients, i.e. now they depend on the additional ACD parameter, the inverse of the compactification radius R. At large values of $1/R$ SM phenomenology should be recovered, since the new states, being more and more massive, are decoupled from the low energy theory.

Now the modified Wilson coefficients in the ACD model contain the contribution from new particles that are not present in the SM and come as an intermediate state in penguin and box diagrams. Thus, these coefficients can be expressed in terms of the functions $F(x_t, 1/R)$, $x_t = \frac{m_t^2}{M_W^2}$, which generalize the corresponding SM function $F_0(x_t)$ according to

$$F(x_t, 1/R) = F_0(x_t) + \sum_{n=1}^{\infty} F_n(x_t, x_n)\,, \tag{5}$$

with $x_n = \frac{m_n^2}{M_W^2}$ and $m_n = \frac{n}{R}$ [13]. The relevant diagrams are Z^0 penguins, γ penguins, gluon penguins, γ magnetic penguins, chromomagnetic penguins and the corresponding functions are $C(x_t, 1/R)$, $D(x_t, 1/R)$, $E(x_t, 1/R)$, $D'(x_t, 1/R)$ and $E'(x_t, 1/R)$, respectively. These functions can be found in [8,9] and can be summarized as follows.

– C_7

In place of C_7, one defines an effective coefficient $C_7^{(0)\mathrm{eff}}$ which is renormalization scheme independent [22]:

$$C_7^{(0)\mathrm{eff}}(\mu_b) = \eta^{\frac{16}{23}} C_7^{(0)}(\mu_W) + \frac{8}{3}(\eta^{\frac{14}{23}} - \eta^{\frac{16}{23}}) C_8^{(0)}(\mu_W) + C_2^{(0)}(\mu_W) \sum_{i=1}^{8} h_i \eta^{\alpha_i}\,, \tag{6}$$

where $\eta = \frac{\alpha_s(\mu_W)}{\alpha_s(\mu_b)}$, and

$$C_2^{(0)}(\mu_W) = 1\,, \quad C_7^{(0)}(\mu_W) = -\frac{1}{2} D'\left(x_t, \frac{1}{R}\right),$$
$$C_8^{(0)}(\mu_W) = -\frac{1}{2} E'\left(x_t, \frac{1}{R}\right); \tag{7}$$

the superscript (0) is for the leading logarithm approximation. Furthermore,

$$\begin{aligned}
\alpha_1 &= \frac{14}{23}\,, & \alpha_2 &= \frac{16}{23}\,,\\
\alpha_3 &= \frac{6}{23}\,, & \alpha_4 &= -\frac{12}{23}\,,\\
\alpha_5 &= 0.4086\,, & \alpha_6 &= -0.4230\,,\\
\alpha_7 &= -0.8994\,, & \alpha_8 &= -0.1456\,,\\
h_1 &= 2.996\,, & h_2 &= -1.0880\,,\\
h_3 &= -\frac{3}{7}\,, & h_4 &= -\frac{1}{14}\,,\\
h_5 &= -0.649\,, & h_6 &= -0.0380\,,\\
h_7 &= -0.0185\,, & h_8 &= -0.0057\,.
\end{aligned} \tag{8}$$

The functions D' and E' are given by (8) with

$$D_0'(x_t) = -\frac{\left(8x_t^3 + 5x_t^2 - 7x_t\right)}{12\left(1-x_t\right)^3} + \frac{x_t^2\left(2-3x_t\right)}{2\left(1-x_t\right)^4}\ln x_t\,, \tag{9}$$

$$E_0'(x_t) = -\frac{x_t\left(x_t^2 - 5x_t - 2\right)}{4\left(1-x_t\right)^3} + \frac{3x_t^2}{2\left(1-x_t\right)^4}\ln x_t\,, \tag{10}$$

$$\begin{aligned}
D_n'(x_t, x_n) = {} & \left[x_t\left(-37 + 44x_t + 17x_t^2 + 6x_n^2\left(10 - 9x_t + 3x_t^2\right)\right.\right.\\
& \left.\left. -3x_n\left(21 - 54x_t + 17x_t^2\right)\right)\right]\frac{1}{36\left(x_t-1\right)^3}\\
& + \frac{x_n\left(2 - 7x_n + 3x_n^2\right)}{6}\ln\frac{x_n}{1+x_n}\\
& - \left[(-2 + x_n + 3x_t)\right.\\
& \quad \times \left(x_t + 3x_t^2 + x_n^2\left(3 + x_t\right)\right.\\
& \quad \left.\left. -x_n\left(1 + (-10 + x_t)\,x_t\right)\right)\right]\frac{1}{6\left(x_t-1\right)^4}\\
& \times \ln\frac{x_n + x_t}{1+x_n}\,,
\end{aligned} \tag{11}$$

$$\begin{aligned}
E_n'(x_t, x_n) = {} & \left[x_t\left(-17 - 8x_t + x_t^2 + 3x_n\left(21 - 6x_t + x_t^2\right)\right.\right.\\
& \left.\left. -6x_n^2\left(10 - 9x_t + 3x_t^2\right)\right)\right]\frac{1}{12\left(x_t-1\right)^3}\\
& - \frac{1}{2}x_n\left(1+x_n\right)\left(-1 + 3x_n\right)\ln\frac{x_n}{1+x_n}\\
& + \left[\left(1+x_n\right)\left(x_t + 3x_t^2 + x_n^2\left(3 + x_t\right)\right.\right.\\
& \quad \left.\left. -x_n\left(1 + (-10 + x_t)\,x_t\right)\right)\right]\frac{1}{2\left(x_t-1\right)^4}\\
& \times \ln\frac{x_n + x_t}{1+x_n}\,.
\end{aligned} \tag{12, 13}$$

Following [8,9], one gets the expressions for the sum over n:

$$\begin{aligned}
\sum_{n=1}^{\infty} D_n'(x_t, x_n) = {} & -\frac{x_t(-37 + x_t(44 + 17x_t))}{72(x_t-1)^3}\\
& + \frac{\pi M_W R}{2}\left[\int_0^1 \mathrm{d}y \frac{2y^{\frac{1}{2}} + 7y^{\frac{3}{2}} + 3y^{\frac{5}{2}}}{6}\coth(\pi M_W R\sqrt{y})\right.\\
& + \frac{(-2+x_t)x_t(1+3x_t)}{6(x_t-1)^4} J\left(R, -\frac{1}{2}\right)\\
& \left. - \frac{1}{6(x_t-1)^4}[x_t(1+3x_t) - (-2+3x_t)(1+(-10+x_t)x_t)]\right.\\
& \times J\left(R, \frac{1}{2}\right)
\end{aligned}$$

$$
\begin{aligned}
&+\frac{1}{6(x_t-1)^4}[(-2+3x_t)(3+x_t)-(1+(-10+x_t)x_t)]\\
&\times J\left(R,\frac{3}{2}\right)\\
&-\frac{(3+x_t)}{6(x_t-1)^4}J\left(R,\frac{5}{2}\right)\Bigg], \qquad (14)\\
&\sum_{n=1}^{\infty}E'_n(x_t,x_n)=\\
&-\frac{x_t(-17+(-8+x_t)x_t)}{24(x_t-1)^3}\\
&+\frac{\pi M_W R}{2}\Bigg[\int_0^1 \mathrm{d}y(y^{\frac{1}{2}}+2y^{\frac{3}{2}}-3y^{\frac{5}{2}})\coth(\pi M_W R\sqrt{y})\\
&-\frac{x_t(1+3x_t)}{(x_t-1)^4}J\left(R,-\frac{1}{2}\right)\\
&+\frac{1}{(x_t-1)^4}[x_t(1+3x_t)-(1+(-10+x_t)x_t)]\\
&\times J\left(R,\frac{1}{2}\right)\\
&-\frac{1}{(x_t-1)^4}[(3+x_t)-(1+(-10+x_t)x_t)]\\
&\times J\left(R,\frac{3}{2}\right)\\
&+\frac{(3+x_t)}{(x_t-1)^4}J\left(R,\frac{5}{2}\right)\Bigg], \qquad (15)
\end{aligned}
$$

where

$$
\begin{aligned}
&J(R,\alpha)=\\
&\int_0^1 \mathrm{d}y y^{\alpha}\left[\coth(\pi M_W R\sqrt{y})-x_t^{1+\alpha}\coth(\pi m_t R\sqrt{y})\right]. \qquad (16)
\end{aligned}
$$

– C_9

In the ACD model and in the NDR scheme one has

$$
\begin{aligned}
C_9(\mu)=P_0^{\mathrm{NDR}}&+\frac{Y\left(x_t,\frac{1}{R}\right)}{\sin^2\theta_{\mathrm{W}}}-4Z\left(x_t,\frac{1}{R}\right)\\
&+P_E E\left(x_t,\frac{1}{R}\right), \qquad (17)
\end{aligned}
$$

where $P_0^{\mathrm{NDR}}=2.60\pm0.25$ [22] and the last term is numerically negligible. Besides

$$
\begin{aligned}
Y\left(x_t,\frac{1}{R}\right)&=Y_0(x_t)+\sum_{n=1}^{\infty}C_n(x_t,x_n),\\
Z\left(x_t,\frac{1}{R}\right)&=Z_0(x_t)+\sum_{n=1}^{\infty}C_n(x_t,x_n), \qquad (18)
\end{aligned}
$$

with

$$
\begin{aligned}
Y_0(x_t)&=\frac{x_t}{8}\left[\frac{x_t-4}{x_t-1}+\frac{3x_t}{(x_t-1)^2}\ln x_t\right],\\
Z_0(x_t)&=\frac{18x_t^4-163x_t^3+259x_t^2-108x_t}{144(x_t-1)^3}\\
&\quad+\left[\frac{32x_t^4-38x_t^3+15x_t^2-18x_t}{72(x_t-1)^4}-\frac{1}{9}\right]\ln x_t, \qquad (19)\\
C_n(x_t,x_n)&=\frac{x_t}{8(x_t-1)^2}\Bigg[x_t^2-8x_t+7\\
&\quad+(3+3x_t+7x_n-x_tx_n)\ln\frac{x_t+x_n}{1+x_n}\Bigg] \qquad (20)
\end{aligned}
$$

and

$$
\begin{aligned}
\sum_{n=1}^{\infty}C_n(x_t,x_n)&=\frac{x_t(7-x_t)}{16(x_t-1)}-\frac{\pi M_W R x_t}{16(x_t-1)^2}\\
&\quad\times\left[3(1+x_t)J\left(R,-\frac{1}{2}\right)+(x_t-7)J\left(R,\frac{1}{2}\right)\right]. \qquad (21)
\end{aligned}
$$

– C_{10}

C_{10} is μ independent and is given by

$$
C_{10}=-\frac{Y\left(x_t,\frac{1}{R}\right)}{\sin^2\theta_{\mathrm{W}}}. \qquad (22)
$$

The normalization scale is fixed to $\mu=\mu_b\simeq 5$ GeV.

3 Decay rate and forward–backward asymmetry

It is well known that Wilson coefficients give short distance effects whereas long distance effects involve the matrix elements of the operators in (2) between the B and K_1 mesons in $B\to K_1\tau^+\tau^-$. Using a standard parameterization in terms of the form factors we have [31]

$$
\begin{aligned}
\langle K_1(k,\varepsilon)|V_\mu|B(p)\rangle&=\mathrm{i}\varepsilon_\mu^*(M_B+M_{K_1})V_1(s)\\
&\quad-(p+k)_\mu(\varepsilon^*\cdot q)\frac{V_2(s)}{M_B+M_{K_1}}\\
&\quad-q_\mu(\varepsilon^*\cdot q)\frac{2M_{K_1}}{s}[V_3(s)-V_0(s)], \qquad (23)\\
\langle K_1(k,\varepsilon)|A_\mu|B(p)\rangle&=\frac{2\mathrm{i}\epsilon_{\mu\nu\alpha\beta}}{M_B+M_{K_1}}\varepsilon^{*\nu}p^\alpha k^\beta A(s), \qquad (24)
\end{aligned}
$$

where $V_\mu=\bar{s}\gamma_\mu b$ and $A_\mu=\bar{s}\gamma_\mu\gamma_5 b$ are the vector and axial vector currents, respectively, and ε_μ^* is the polarization vector for the final state axial vector meson.

The relationship between the different form factors, which also ensures that there is no kinematical singularity in the matrix element at $s=0$, is

$$
\begin{aligned}
V_3(s)&=\frac{M_B+M_{K_1}}{2M_{K_1}}V_1(s)-\frac{M_B-M_{K_1}}{2M_{K_1}}V_2(s), \qquad (25)\\
V_3(0)&=V_0(0). \qquad (26)
\end{aligned}
$$

In addition to the above form factors there are also some penguin form factors:

$$\begin{aligned}
&\langle K_1(k,\varepsilon)|\bar{s}\mathrm{i}\sigma_{\mu\nu}q^\nu b|B(p)\rangle = \\
&\quad\big[\big(M_B^2 - M_{K_1}^2\big)\varepsilon_\mu^* - (\varepsilon^*\cdot q)(p+k)_\mu\big]F_2(s) \\
&\quad + (\varepsilon^*\cdot q)\bigg[q_\mu - \frac{s}{M_B^2 - M_{K_1}^2}(p+k)_\mu\bigg]F_3(s)\,, \qquad (27)\\
&\langle K_1(k,\varepsilon)|\bar{s}\mathrm{i}\sigma_{\mu\nu}q^\nu\gamma_5 b|B(p)\rangle = -\mathrm{i}\epsilon_{\mu\nu\alpha\beta}\varepsilon^{*\nu}p^\alpha k^\beta F_1(s)\,, \qquad (28)
\end{aligned}$$

with $F_1(0) = 2F_2(0)$.

Form factors are non-perturbative quantities and are scalar functions of the square of the momentum transfer. Different models are used to calculate these form factors. The form factors we use here in the analysis of observables like the decay rate, forward–backward asymmetry and polarization asymmetries of the final state τ in $B \to K_1\tau^+\tau^-$ have been calculated using Ward identities. The detailed calculation and their expressions are given in [31] and can be summarized as

$$\begin{aligned}
A(s) &= \frac{A(0)}{\big(1 - s/M_B^2\big)\big(1 - s/M_B'^2\big)}\,,\\
V_1(s) &= \frac{V_1(0)}{\big(1 - s/M_{B_A^*}^2\big)\big(1 - s/M_{B_A^*}'^2\big)}\bigg(1 - \frac{s}{M_B^2 - M_{K_1}^2}\bigg)\,,\\
V_2(s) &= \frac{\tilde{V}_2(0)}{\big(1 - s/M_{B_A^*}^2\big)\big(1 - s/M_{B_A^*}'^2\big)} \\
&\quad - \frac{2M_{K_1}}{M_B - M_{K_1}}\frac{V_0(0)}{\big(1 - s/M_B^2\big)\big(1 - s/M_B'^2\big)}\,, \qquad (29)
\end{aligned}$$

with

$$\begin{aligned}
A(0) &= -(0.52 \pm 0.05)\,,\\
V_1(0) &= -(0.24 \pm 0.02)\,,\\
\tilde{V}_2(0) &= -(0.39 \pm 0.03)\,. \qquad (30)
\end{aligned}$$

The corresponding values for the $B \to K^*$ form factors at $s = 0$ are given by [14]

$$\begin{aligned}
V(0) &= (0.29 \pm 0.04)\,,\\
A_1(0) &= (0.23 \pm 0.03)\,,\\
\tilde{A}_2(0) &= (0.33 \pm 0.05)\,. \qquad (31)
\end{aligned}$$

Following the notation of [19], the differential decay rate in terms of the auxiliary functions can be written as

$$\frac{\mathrm{d}\Gamma}{\mathrm{d}s} = \frac{G_\mathrm{F}^2|V_{tb}V_{ts}^*|^2\alpha^2}{2^{11}\pi^5}\frac{\lambda^{1/2}\big(M_B^2, M_{K_1}^2, s\big)}{3M_B^3M_{K_1}^2 s}\sqrt{1 - \frac{4m_\tau^2}{s}}\,g(s)\,, \qquad (32)$$

where $\lambda(a,b,c) = a^2 + b^2 + c^2 - 2ab - 2bc - 2ca$ and the function $g(s)$ is

$$\begin{aligned}
g(s) &= 24|D_0|^2m_\tau^2M_{K_1}^2\lambda \\
&\quad + 8sM_{K_1}^2\lambda\left[\big(2m_\tau^2 + s\big)|A|^2 - \big(4m_\tau^2 - s\big)|C|^2\right] \\
&\quad + \lambda\left[\big(2m_\tau^2 + s\big)\big|B_1 + \big(M_B^2 - M_{K_1}^2 - s\big)B_2\big|^2\right. \\
&\quad \left. - \big(4m_\tau^2 - s\big)\big|D_1 + \big(M_B^2 - M_{K_1}^2 - s\big)D_2\big|^2\right] \\
&\quad + 4sM_{K_1}^2\left[\big(2m_\tau^2 + s\big)\big(3|B_1|^2 - \lambda|B_2|^2\big)\right. \\
&\quad \left. - \big(4m_\tau^2 - s\big)\big(3|D_1|^2 - \lambda|D_2|^2\big)\right]\,. \qquad (33)
\end{aligned}$$

The auxiliary functions contain the short distance contribution (Wilson coefficients) as well as the long distance contribution (form factors):

$$\begin{aligned}
A &= 4(m_b + m_s)\frac{C_7^\mathrm{eff}}{s}F_1(s) - \frac{A_0(s)}{M_B + M_{K_1}}C_9^\mathrm{eff}(s)\,,\\
B_1 &= (M_B + M_{K_1})\bigg[C_9^\mathrm{eff}(s)V_1(s) \\
&\quad + \frac{4m_b}{s}C_7^\mathrm{eff}(M_B - M_{K_1})F_2(s)\bigg]\,,\\
B_2 &= -\bigg[\frac{4m_b}{s}C_7^\mathrm{eff}\bigg(F_2(s) + s\frac{F_3(s)}{M_B^2 - M_{K_1}^2}\bigg) \\
&\quad + C_9^\mathrm{eff}(s)\frac{V_2(s)}{M_B + M_{K_1}}\bigg]\,,\\
C &= -C_{10}\frac{A(s)}{M_B + M_{K_1}}\,,\\
D_0 &= C_{10}V_0(s)\,,\\
D_1 &= C_{10}V_1(s)(M_B + M_{K_1})\,,\\
D_2 &= C_{10}\frac{V_2(s)}{M_B + M_{K_1}}\,. \qquad (34)
\end{aligned}$$

Thus, integrating (32) over s and using the value of the form factors defined in (29), the numerical value of the branching ratio $B \to K_1\tau^+\tau^-$ is

$$B(B \to K_1\tau^+\tau^-) = (0.06 \pm 0.01) \times 10^{-7}.$$

The error in the value reflects the uncertainty from the form factors, and it is due to the variation of input parameters like the CKM matrix elements, the decay constant of B meson and the masses as defined in Table 1.

Table 1. Default values of input parameters used in the calculation

m_W	80.41 GeV
m_Z	91.1867 GeV
$\sin^2\theta_\mathrm{W}$	0.2233
m_c	1.4 GeV
$m_{b,\mathrm{pole}}$	4.8 ± 0.2 GeV
m_t	173.8 ± 5.0 GeV
$\alpha_\mathrm{s}(m_Z)$	0.119 ± 0.0058
f_B	(200 ± 30) MeV
$\lvert V_{ts}^*V_{tb}\rvert$	0.0385

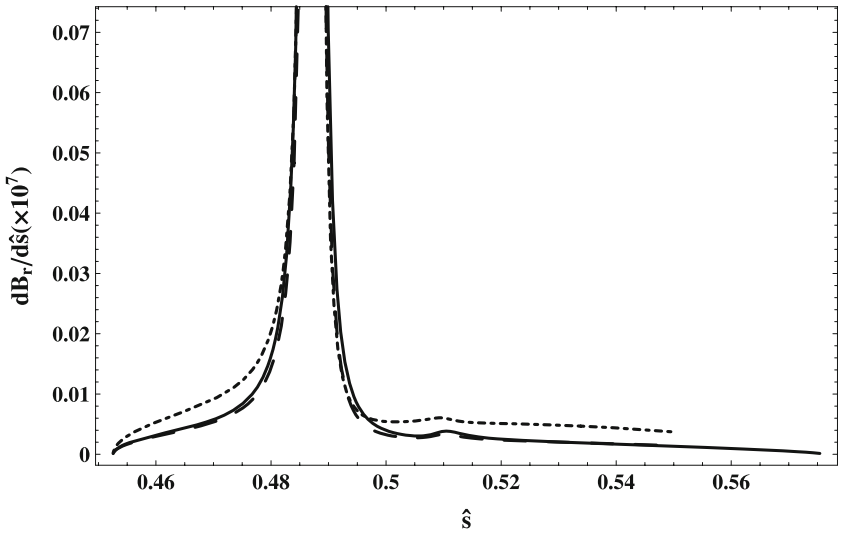

Fig. 1. The differential branching ratio as a function of $\hat{s}$ is plotted using the form factors defined in (29). The *solid line* denotes the SM result, the *dashed-dotted line* is for $1/R = 200\,\text{GeV}$ and the *dashed line* is for $1/R = 500\,\text{GeV}$. All the input parameters are taken at their central values

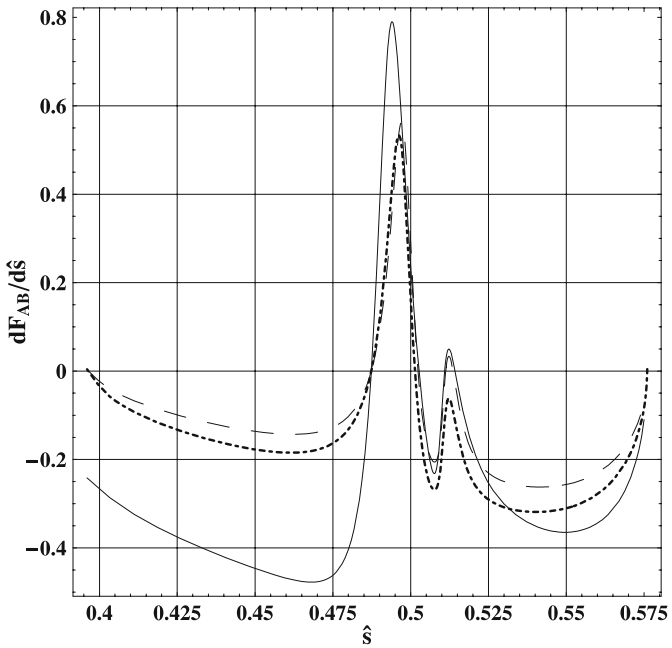

Fig. 2. The differential forward–backward (FB) asymmetry as a function of $\hat{s}$ is plotted using the form factors defined in (29). The *solid line* denotes the SM result, the *dashed line* is for $1/R = 200\,\text{GeV}$ and the *dashed-dotted line* is for $1/R = 500\,\text{GeV}$. All the input parameters are taken at their central values

It has already been mentioned that in the ACD model there is no new operator beyond the SM and new physics will come only through the Wilson coefficients. To see this, the differential branching ratio against $\hat{s}(= s/M_B^2)$ is plotted in Fig. 1 using the central values of the input parameters. One can see that the effects of the KK contribution in the Wilson coefficient are modest for $1/R = 200\,\text{GeV}$ at low value of $\hat{s}$ but such effects are obscured by the uncertainties involved in different parameters like the form factors, CKM matrix elements, etc. at large values of $\hat{s}$.

Another observable is the forward–backward asymmetry ($\mathcal{A}_{\text{FB}}$), which also is a very useful tool for looking for new physics. It has been shown by Ishtiaq et al. [14] that the zero of the forward–backward asymmetry is considerably shifted to the left in the ACD model for $B \to K_1\mu^+\mu^-$. We have shown in Fig. 2 the differential forward–backward asymmetry with $\hat{s}$ for $B \to K_1\tau^+\tau^-$. Again the sensitivity of the zero on the extra dimension is very mild for $1/R = 200\,\text{GeV}$.

4 Polarization asymmetries of final state leptons

In this section we will discuss the final state lepton polarization asymmetries by following the notation defined in [19]. To compute these for B decays in τ leptons we consider the spin vector n of τ^-, with $n^2 = -1$ and $\mathbf{k}_1 \cdot n = 0$, and $\mathbf{k}_1$ is the momentum of τ^-. Now in the rest frame of the τ^- lepton, one can define the three orthogonal unit vectors e_{L}, e_{N} and e_{T} corresponding to the longitudinal, n_{L}, normal, n_{N}, and transverse, n_{T}, polarization vectors:

$$
\begin{aligned}
n_{\text{L}} &= (0, e_{\text{L}}) = \left(0, \frac{\mathbf{k}_1}{|\mathbf{k}_1|}\right), \\
n_{\text{N}} &= (0, e_{\text{N}}) = \left(0, \frac{\mathbf{p} \times \mathbf{k}_1}{|\mathbf{p} \times \mathbf{k}_1|}\right), \\
n_{\text{T}} &= (0, e_{\text{T}}) = (0, e_{\text{N}} \times e_{\text{T}}),
\end{aligned} \tag{35}
$$

where $\mathbf{p}$ and $\mathbf{k}_1$ are the three momenta of K_1 and τ^- in the rest frame of the lepton pair. If we choose the z-axis as the momentum direction of τ^- in the rest frame of the lepton pair, then $k_1 = (E_1, 0, 0, |\mathbf{k}_1|)$. Now boosting the spin vector n defined in (35) in the rest frame of the lepton pair, the normal and transverse vectors n_{N} and n_{T} remain unchanged, but the longitudinal polarization vectors change. Their new forms become

$$
\begin{aligned}
n_{\text{N}} &= (0, 1, 0, 0), \\
n_{\text{T}} &= (0, 0, -1, 0),
\end{aligned}
$$

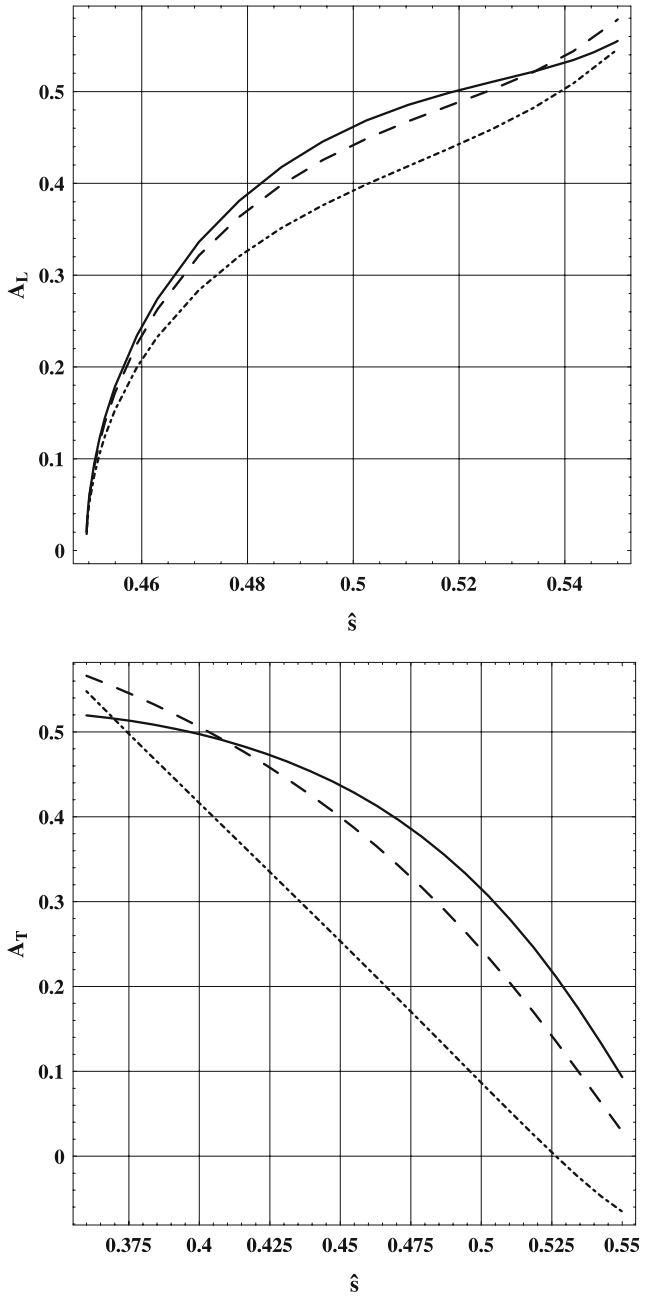

Fig. 3. Longitudinal (*upper panel*) and transverse (*lower panel*) τ^- polarization asymmetry in $B \to K_1\tau^-\tau^+$ is plotted as a function of $\hat{s}$ using form factor defined in (29). The *solid line* denotes the SM result, the *dashed line* is for $1/R = 200$ GeV and the *long-dashed line* is for $1/R = 500$ GeV. All the input parameters are taken at their central values

$$n_{\rm L} = \frac{1}{m_\tau}(|\mathbf{k}_1|, 0, 0, E_1)\,. \tag{36}$$

The polarization asymmetry for a negatively charged lepton τ^- for each value of the square of momentum transfer to the lepton pairs, s, can be defined by

$$\mathcal{A}_i(s) = \frac{\frac{{\rm d}\Gamma}{{\rm d}s}(n_i) - \frac{{\rm d}\Gamma}{{\rm d}s}(-n_i)}{\frac{{\rm d}\Gamma}{{\rm d}s}(n_i) + \frac{{\rm d}\Gamma}{{\rm d}s}(-n_i)}\,, \tag{37}$$

with $i = {\rm L}$, T and N.

Thus, for $B \to K_1\tau^+\tau^-$ the expression of the longitudinal, $\mathcal{A}_{\rm L}(s)$, and transverse, $\mathcal{A}_{\rm T}(s)$, polarization asymmetries of τ^- becomes [19]

$$\begin{aligned}\mathcal{A}_{\rm L}(s) = 2s\sqrt{1-\frac{4m_\tau^2}{s}}\frac{1}{g(s)}\big\{&8sM_{K_1}^2\,{\rm Re}[B_1D_1^* + \lambda AC^*] \\ &+ {\rm Re}\left[\left(M_B^2 - M_{K_1}^2 - s\right)B_1 + \lambda B_2\right] \\ &\times \left[\left(M_B^2 - M_{K_1}^2 - s\right)D_1^* + \lambda D_2^*\right]\big\}\,, \end{aligned} \tag{38}$$

$$\begin{aligned}\mathcal{A}_{\rm T}(s) = 3\pi m_\tau M_{K_1}\frac{\lambda\sqrt{s}}{g(s)}\big\{&-4\,{\rm Re}[AB_1^*]M_{K_1}s \\ &+ {\rm Re}\left[D_0B_1^*\left(M_B^2 - M_{K_1}^2 - s\right) + \lambda D_0B_2^*\right]\big\}\,, \end{aligned} \tag{39}$$

with $\lambda = \lambda(M_B^2, M_{K_1}^2, s)$. Now, while calculating these asymmetries we do not consider the contribution associated with the real $c\bar{c}$ resonances in $C_9^{\rm eff}$, as these can be removed by using appropriate kinematical cuts [19]. It is clear from (38) that the value of the longitudinal polarization asymmetry vanishes when $s = 4m_\tau^2$. In Fig. 3 we have shown the effect of the extra dimension on the value of the asymmetries. One can see that the longitudinal polarization has the largest value at large momentum transfer (large value of $\hat{s}$) and is least sensitive to the compactification radius $1/R$. The effects of the extra dimension are more evident for the transverse polarization, whose value decreases with the decrease of $1/R$ down to $1/R = 200$, and the change is maximum for a low value of $\hat{s}$.

5 Helicity fractions of K_1 in $B \to K_1\ell^+\ell^-$

In this section, we study the helicity fractions of the K_1 produced in the final state, which is another interesting variable. For the K^* meson, the longitudinal helicity fraction $f_{\rm L}$ in the modes $B \to K^*\ell^+\ell^-$ $(\ell = e, \mu)$, has been measured by the BaBar Collaboration in two bins of momentum transfer [32]. The results are

$$\begin{aligned} f_{\rm L} &= 0.77^{+0.63}_{-0.30} \pm 0.07\,, \quad 0.1\,{\rm GeV}^2 \le s \le 8.41\,{\rm GeV}^2\,, \\ f_{\rm L} &= 0.51^{+0.22}_{-0.25} \pm 0.08\,, \qquad\qquad s \ge 10.24\,{\rm GeV}^2\,, \end{aligned} \tag{40}$$

while the average value of $f_{\rm L}$ in the full s range is [19]

$$f_{\rm L} = 0.63^{+0.18}_{-0.19} \pm 0.05\,, \qquad s \ge 0.1\,{\rm GeV}^2\,. \tag{41}$$

The expressions of the $B \to K^*\ell^+\ell^-$ differential decays widths with K^* longitudinal (L) or transversely ($\pm$) polarized are calculated by Colangelo et al. [19]. We will translate the same results for $B \to K_1\ell^+\ell^-$ as K^* and K_1 differ by γ_5 in their distribution amplitudes. The result reads

$$\begin{aligned}\frac{{\rm d}\Gamma_{\rm L}(s)}{{\rm d}s} = \frac{G_{\rm F}^2|V_{tb}V_{ts}^*|^2\alpha^2}{2^{11}\pi^5}\frac{\lambda^{1/2}\left(M_B^2, M_{K_1}^2, s\right)}{M_B^3} \\ \times\sqrt{1-\frac{4m_\ell^2}{s}}\frac{1}{3}A_{\rm L}\,, \end{aligned}$$

$$\frac{\mathrm{d}\Gamma_+(s)}{\mathrm{d}s} = \frac{G_\mathrm{F}^2 |V_{tb}V_{ts}^*|^2 \alpha^2}{2^{11}\pi^5} \frac{\lambda^{1/2}\big(M_B^2, M_{K_1}^2, s\big)}{M_B^3} \times \sqrt{1-\frac{4m_\ell^2}{s}} \frac{4}{3} A_+ ,$$
$$\frac{\mathrm{d}\Gamma_-(s)}{\mathrm{d}s} = \frac{G_\mathrm{F}^2 |V_{tb}V_{ts}^*|^2 \alpha^2}{2^{11}\pi^5} \frac{\lambda^{1/2}\big(M_B^2, M_{K_1}^2, s\big)}{M_B^3} \times \sqrt{1-\frac{4m_\ell^2}{s}} \frac{4}{3} A_- , \quad (42)$$

with

$$A_\mathrm{L} = \frac{1}{sM_{K_1}^2} \Big\{ 24|D_0|^2 m_\ell^2 M_{K_1}^2 \lambda + \big(2m_\ell^2 + s\big)\big|\big(M_B^2 - M_{K_1}^2 - s\big)B_1 + \lambda B_2\big|^2 + \big(s - 4m_\ell^2\big)\big|\big(M_B^2 - M_{K_1}^2 - s\big)D_1 + \lambda D_2\big|^2 \Big\} \quad (43)$$

and

$$A_- = \big(s-4m_\ell^2\big)\big|D_1 + \lambda^{1/2} C\big|^2 + \big(s+2m_\ell^2\big)\big|B_1 + \lambda^{1/2} A\big|^2 ,$$
$$A_+ = \big(s-4m_\ell^2\big)\big|D_1 - \lambda^{1/2} C\big|^2 + \big(s+2m_\ell^2\big)\big|B_1 - \lambda^{1/2} A\big|^2 . \quad (44)$$

The auxiliary functions and the corresponding form factors are defined in (34) and (30). The various helicity amplitudes are defined as [19]

$$f_\mathrm{L}(s) = \frac{\mathrm{d}\Gamma_\mathrm{L}(s)/\mathrm{d}s}{\mathrm{d}\Gamma(s)/\mathrm{d}s} ,$$
$$f_\pm(s) = \frac{\mathrm{d}\Gamma_\pm(s)/\mathrm{d}s}{\mathrm{d}\Gamma(s)/\mathrm{d}s} ,$$
$$f_\mathrm{T}(s) = f_+(s) + f_-(s) . \quad (45)$$

The helicity fractions for K^* have been considered in the SM and some of its extensions [19, 33]. In Fig. 4 we have shown the results of the helicity fractions of K^* using the central value of the form factors and other parameters defined in [14] in the SM and for two values of the

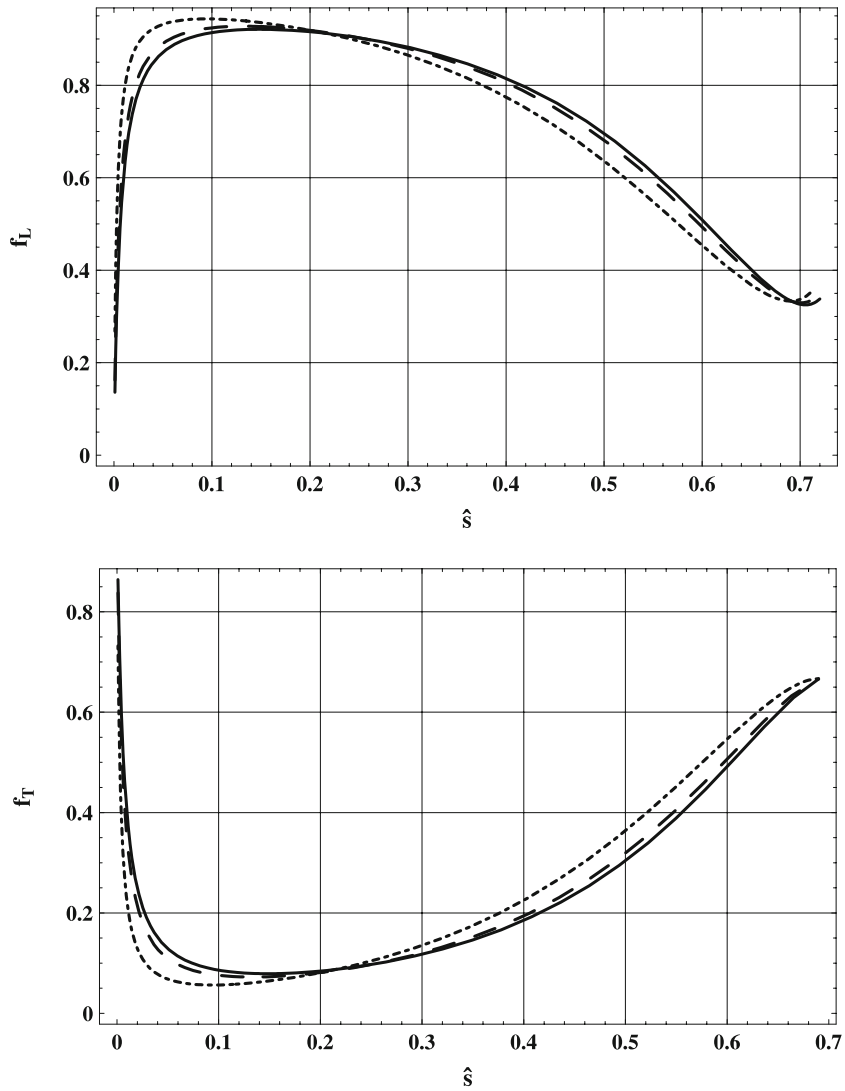

Fig. 4. Longitudinal (*upper panel*) and transverse (*lower panel*) K^* helicity fractions in $B \to K^* \ell^- \ell^+$ ($\ell = e, \mu$) are obtained using form factor defined in (31). The *solid line* denotes the SM result, the *dashed line* is for $1/R = 200$ GeV and the *long-dashed line* is for $1/R = 500$ GeV. All the input parameters are taken at their central values

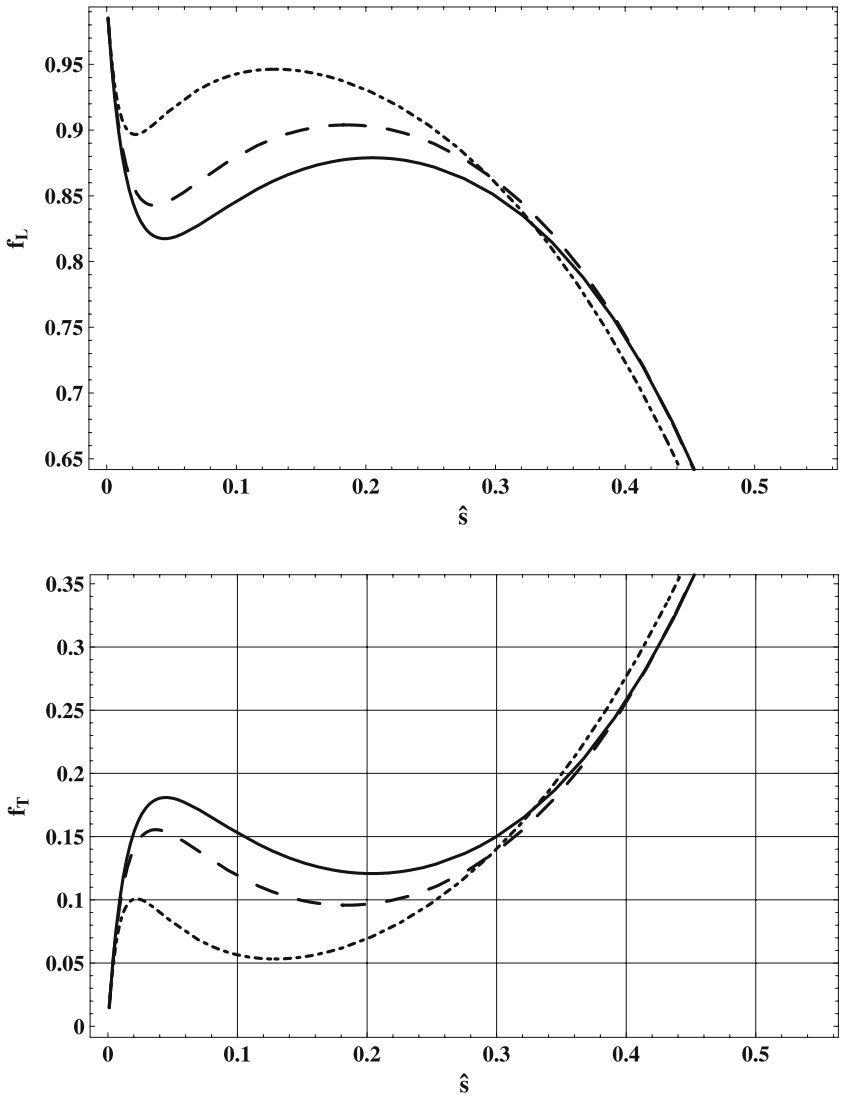

Fig. 5. Longitudinal (*upper panel*) and transverse (*lower panel*) K_1 helicity fractions in $B \to K_1\ell^-\ell^+$ $(\ell = e, \mu)$ are obtained using form factor defined in (29). The *solid line* denotes the SM result, the *dashed line* is for $1/R = 200\,\text{GeV}$ and the *long-dashed line* is for $1/R = 500\,\text{GeV}$. All the input parameters are taken at their central values

compactification radius $1/R$. The lepton in the final state is considered to be e or μ. The effects of the extra dimensions are very mild for low values of the momentum transfer. One can see that the value of the longitudinal helicity agrees with the experimental data within the experimental uncertainties both for small and large values of the momentum transfer. Thus, measurement of the transverse helicity fraction will discriminate between the different models [19].

The results for the case of K_1 are shown in Figs. 5 and 6 in the SM and in the UED model for two values of $1/R$. Figure 5 shows the helicity fractions of K_1 when we consider the e and μ as the final state lepton in $B \to K_1\ell^+\ell^-$ and take all the input parameters at their central values. One can see that the effects of the extra dimension are very prominent at small values of the momentum transfer. These effects are constructive for the case of the transverse helicity fraction and destructive for the longitudinal one. Similarly, Fig. 6 depicts the results when we have considered the τ in the final state. Again, the effects of the extra dimension are very modest at small values of the momentum transfers $\hat{s}$, where f_L is maximum and f_T is minimum. From these two figures it is also clear that at each value of the momentum transfer, $f_L(\hat{s}) + f_T(\hat{s}) = 1$. Thus, we may say that measurement of the helicity fractions of K_1 will be possible in future B factories.

6 Conclusion

In this paper, we have analyzed the spin effects in the semileptonic decay $B \to K_1\tau^+\tau^-$ both in the SM and in the ACD model, which is a minimal extension of the SM with only one extra dimension. We studied the dependence of physical observables like the decay rate, forward–backward asymmetry and polarization asymmetry on the inverse of the compactification radius $1/R$. The effects of the extra dimension on these observables are very mild, but still observable. Among the polarization asymmetries the one most sensitive is the transverse one, where the effects of the extra dimension for $1/R = 200\,\text{GeV}$ are very clear in the low momentum transfer range. The K^* he-

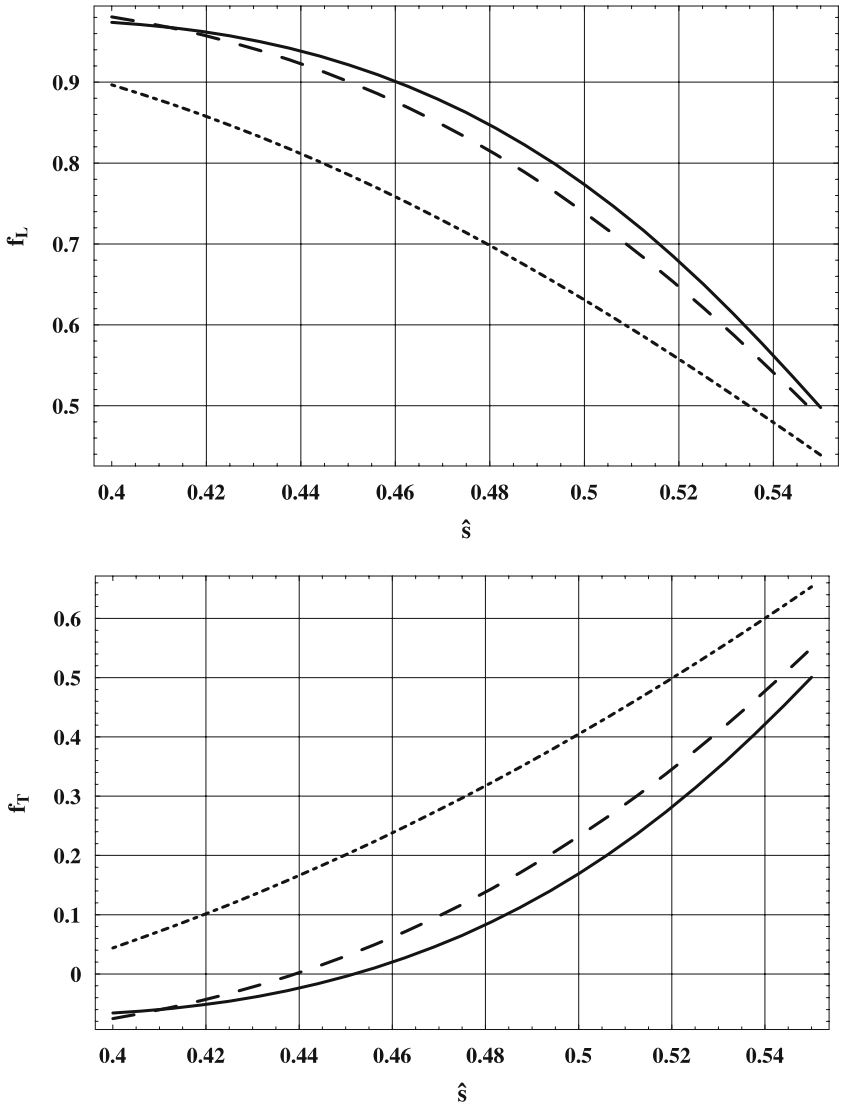

Fig. 6. Longitudinal (*upper panel*) and transverse (*lower panel*) K_1 helicity fractions in $B \to K_1\tau^-\tau^+$ are obtained using form factor defined in (29). The *solid line* denotes the SM result, the *dashed line* is for $1/R = 200$ GeV and the *long-dashed line* is for $1/R = 500$ GeV. All the input parameters are taken at their central values

licity fractions, for which some results for e and μ in the final state are already available, have also been discussed and compared with the existing results in the literature. Finally, following the same analogy we considered the K_1 helicity fractions both in the SM and in the ACD model. It is quite clear that the effects of extra dimensions in all these observables are more evident for lower values of $1/R$. For higher values of the inverse of the compactification radius, like the one mentioned in [18], these extra dimension effects are overshadowed by the hadronic uncertainties involved in these decays. Thus, future experiments, where more data are expected, will put stringent constraints on the compactification radius and also give us deep understanding of B-physics and take us a step forward towards the ultimate theory of the fundamental interactions.

Acknowledgements. This work of Jamil and Lu is partly supported by the National Science Foundation of China under Grants No. 10735080 and 10625525. One of us (Asif) would like to thank Riazuddin, Fayyazuddin, Ishtiaq and Ali for useful discussions.

References

1. I. Antoniadis, Phys. Lett. B **246**, 377 (1990)
2. K.R. Dienes, E. Dudas, T. Gherghetta, Phys. Lett. B **436**, 55 (1998)
3. N. Arkani-Hamed, M. Schmaltz, Phys. Rev. D **61**, 033 005 (2000)
4. N. Arkani-Hamed, S. Dimopoulos, G.R. Dvali, Phys. Lett. B **429**, 263 (1998)
5. L. Randall, R. Sundrum, Phys. Rev. Lett. **83**, 3370 (1999)
6. L. Randall, R. Sundrum, Phys. Rev. Lett. **83**, 4690 (1999)
7. T. Appelquist, H.C. Cheng, B.A. Dobrescu, Phys. Rev. D **64**, 035 002 (2001)
8. A.J. Buras, M. Spranger, A. Weiler, Nucl. Phys. B **660**, 225 (2003)
9. A.J. Buras, A. Poschenrieder, M. Spranger, A. Weiler, Nucl. Phys. B **678**, 455 (2004)

10. S.L. Glashow, J. Iliopoulos, L. Maiani, Phys. Rev. D **2**, 1285 (1970)
11. K. Agashe, N.G. Deshpande, G.H. Wu, Phys. Lett. B **514**, 309 (2001)
12. T. Appelquist, H.U. Yee, Phys. Rev. D **67**, 055 002 (2003)
13. P. Colangelo, F. De Fazio, R. Ferrandes, T.N. Pham, Phys. Rev. D **73**, 115 006 (2006)
14. A. Ishtiaq, M. Ali Paracha, M. Jamil Aslam, arXiv: 0802.0740 [hep-ph]
15. R. Mohanta, A.K. Giri, Phys. Rev. D **75**, 035 008 (2007) [arXiv:hep-ph/0611068]
16. T.M. Aliev, M. Savci, arXiv:hep-ph/0606225
17. T.M. Aliev, M. Savci, B.B. Sirvanli, arXiv:hep-ph/0608143
18. U. Haisch, A. Weiler, Phys. Rev. D **76**, 034 014 (2007) [arXiv:hep-ph/0703064]
19. P. Colangelo, F. De Fazio, R. Ferrandes, T.N. Pham, Phys. Rev. D **74**, 115 006 (2006) [arXiv:hep-ph/0610044]
20. J.L. Hewett, Phys. Rev. D **53**, 4964 (1996)
21. A. Ali, P. Ball, L.T. Handoko, G. Hiller, Phys. Rev. D **61**, 074 024 (2000) [arXiv:hep-ph/9910221]
22. A.J. Buras et al., Nucl. Phys. B **424**, 374 (1994)
23. C. Bobeth, M. Misiak, J. Urban, Nucl. Phys. B **574**, 291 (2000)
24. H.H. Asatrian, H.M. Asatrian, C. Greub, M. Walker, Phys. Lett. B **507**, 162 (2001)
25. H.H. Asatrian, H.M. Asatrian, C. Greub, M. Walker, Phys. Rev. D **65**, 074 004 (2002)
26. H.H. Asatrian, H.M. Asatrian, C. Greub, M. Walker, Phys. Rev. D **66**, 034 009 (2002)
27. H.M. Asatrian, K. Bieri, C. Greub, A. Hovhannisyan, Phys. Rev. D **66**, 094 013 (2002)
28. A. Ghinculov, T. Hurth, G. Isidori, Y.P. Yao, Nucl. Phys. B **648**, 254 (2003)
29. A. Ghinculov, T. Hurth, G. Isidori, Y.P. Yao, Nucl. Phys. B **685**, 351 (2004)
30. C. Bobeth, P. Gambino, M. Gorbahn, U. Haisch, JHEP **0404**, 071 (2004)
31. M. Ali Paracha, A. Ishtiaq, M. Jamil Aslam, Eur. Phys. J. C **52**, 967 (2007)
32. BaBar Collaboration, B. Aubert et al., Phys. Rev. D **73**, 092 001 (2006)
33. T.M. Aliev, A. Ozpineci, M. Savci, Phys. Lett. B **511**, 49 (2001)